Structural Engineering and Mechanics, *Vol. 47, No. 6 (2013) 839-856*
DOI: http://dx.doi.org/10.12989/sem.2013.47.6.839

Effects of thickness variations on the thermal elastoplastic behavior of annular discs

Yun-Che Wang*[1], Sergei Alexandrov[2,3] and Yeau-Ren Jeng[3]

[1]*Department of Civil Engineering, National Cheng Kung University, Tainan 70101, Taiwan*
[2]*A. Ishlinskii Institute for Problems in Mechanics, Russian Academy of Sciences, 119526 Moscow, Russia*
[3]*Department of Mechanical Engineering and Advanced Institute of Manufacturing with High-tech Innovations, National Chung Cheng University, 62102 Chia-Yi, Taiwan*

(Received June 29, 2013, Revised August 21, 2013, Accepted August 31, 2013)

Abstract. Metallic annular discs with their outer boundary fully constrained are studied with newly derived semi-analytical solutions for the effects of thickness variations under thermal loading and unloading. The plane stress and axisymmetric assumptions were adopted, and the thickness of the disk depends on the radius hyperbolically with an exponent n. Furthermore, it is assumed that the stress state is two dimensional and temperature is uniform in the domain. The solutions include the elastic, elastic-plastic and plastic-collapse behavior, depending on the values of temperature. The von Mises type yield criterion is adopted in this work. The material properties, Young's modulus, yield stress and thermal expansion coefficient, are assumed temperature dependent, while the Poisson's ratio is assumed to be temperature independent. It is found that for any n values, if the normalized hole radius a greater than 0.6, the normalized temperature difference between the elastically reversible temperature and plastic collapse temperature is a monotonically decreasing function of inner radius. For small holes, the n values have strong effects on the normalized temperature difference. Furthermore, it is shown that thickness variations may have stronger effects on the strain distributions when temperature-dependent material properties are considered.

Keywords: analytical method; collapse/failure; elasto-plastic; plane stress/strain; yield criterion

1. Introduction

A metallic thin disk under thermal loading and unloading is of particular importance in engineering design. Under cycling loading, residual stress may accumulated in the material, causing pre-mature failure (Withers 2007). Continuum level modeling requires a choice of constitutive relationships. Various plasticity models have been proposed, and they can be viewed as plasticity theorems with different definition of internal variables (Horstemeyer and Bammann 2010). Popular models, such as the Tresca and von Mises yield criterion, are widely adopted in the theoretical and numerical studies to model the mechanical behavior of materials beyond elasticity. In this work, we adopt the von Mises yield criterion for its superiority in modeling metal plasticity.

In the literature, Thompson and Lester (1946) studied the stress in rotating disks under high temperatures. Vivio and Vullo (2010) studied residual stresses in rotating disk having the

*Corresponding author, Associate Professor, E-mail: yunche@mail.ncku.edu.tw

http://www.techno-press.org/?journal=sem&subpage=8 ISSN: 1225-4568 (Print), 1598-6217 (Online)

hyperbolic profile for estimating its service life under overspeeding. In addition, the thermal yield of a rotating hyperbolic disk is discussed (Alujevic *et al*. 1993). The elastic-plastic stress analyses have been conducted in rotating disks without considerations of elevated temperature and thickness variations (You and Zhang 1999, Rees 1999, Gamer 1984). Orcan and Gamer (1994) has also investigated the growth of plastic regions in annular discs with a shrink fit assemblage. Furthermore, Lenard and Haddow (1972) solved the plastic collapse of rotating cylinders with the plain strain assumption. Alexandrov *et al*. (2012) studied residual stresses and pressure dependence on the yield criterion in a thin disk. In addition, anisotropic effects in rotating disk have been analyzed with inclusions of plastic deformation (Alexandrova and Alexandrov 2004). As a closely related research area, Zimmerman and Lutz (1999) studied the thermal stresses in functionally graded material under uniform heating.

Most aforementioned studies in the past do not consider material properties depending on temperature. Temperature-dependent (TD) material properties are important in analyzing the thermal stresses in materials (Noda 1991, Argeso and Eraslan 2008). Neglect of the effects of material properties being functions of temperature may lead to catastrophic failures in engineering. Considerations of temperature-dependent yield strength are widely conducted in the literature (Lippmann 1992, Kovacs 1994, Bengeri and Mack 1994), since the yield strength is a somewhat more sensitive material property when varying temperature. All of these solutions involve intensive numerical treatment, as well as the Tresca yield criterion is adopted. However, none of these works deals with the system of loading and constraints studied in the present paper. Furthermore, in this work, we develop analytical solution with considerations of all material properties to be temperature dependent, except for Poisson's ratio, in the framework of the von Mises yield criterion for elastic-perfectly plastic materials.

In addition, Eraslan (2003) studied the rotating disk with rigid inclusion and nonlinear hardening variable thickness has been studied for its plastic stresses with von Mises yield criterion. With similar ideas, the disk under external pressure has been analyzed (Eraslan *et al*. 2005). In addition, solid disks under concave profiles under rotation have been investigated (Eraslan and Orcan 2002). Furthermore, Eraslan has investigated annular disks with various boundary conditions under rotations. In addition to annular disks, elastic-plastic stress in a disk containing a rigid inclusion has been analyzed (Güven 1998). And, Güven and Altay (1998) has also studied the hardening of a solid disc with confined outer displacement under uniform heating.

Theoretical developments in the annular disk problem under various loading and boundary conditions with different material models have long been conducted to better predict the mechanical behavior of the disk. However, most of the approaches in the literature do not provide analytical solutions for the combined effects of temperature-dependent (TD) material properties and thickness variations. Hence, in this work, analytical solutions, that include the temperature dependent material properties and hyperbolic thickness profiles, are derived under the plane stress assumption with the von Mises type yield criterion. The exact solutions developed here may be of use in benchmark tests for future numerical studies.

2. Theoretical

In this section, the preliminary setup of the mathematical derivation is described in Section 2.1. Subsequently, Section 2.2 contains the elastic solution, Section 2.3 the elastic/plastic stress solution, and Section 2.4 the elastic/plastic strain solution. Finally, in Section 2.5, solutions for

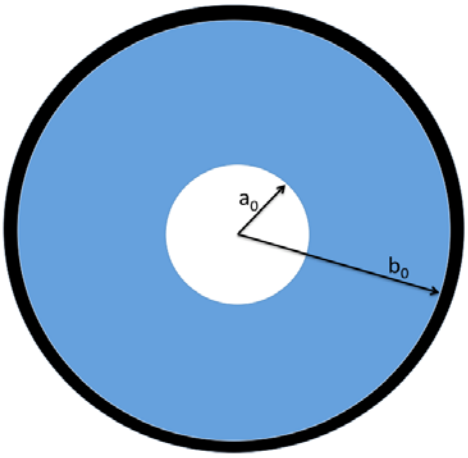

Fig. 1 Schematic of the annular disk (blue) with the inner radius a_0 and outer radius b_0, fully constrained at the outer boundary (thick black)

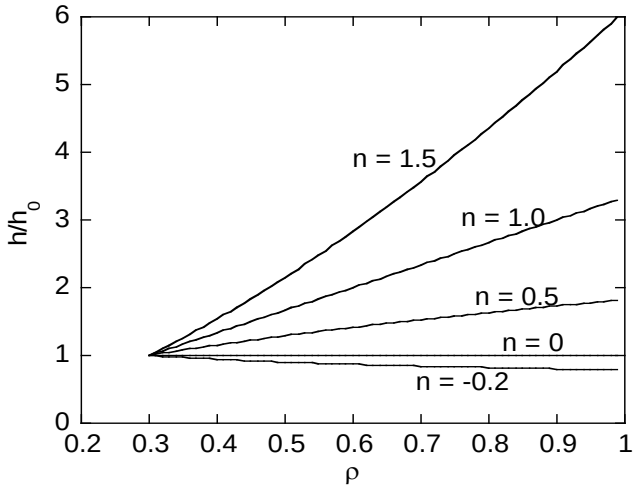

Fig. 2 Thickness profile calculated from Eq. (1)

fully plastic deformation are presented at high temperatures.

2.1 Mathematical setup

It is assumed that the initial thickness (before loading) of the disk varies according to the equation

$$h = h_0 \left(\frac{r}{a_0} \right)^n , \tag{1}$$

where h_0 is the thickness at the inner rim, $r = a_0$, and h the thickness at the outer rim, $r = b_0$, of the

thin hollow elastic-plastic disc, as schematically shown in Fig. 1. The disc is inserted into a rigid container of radius b_0, which provides complete displacement confinement, and subjected to thermal loading by an uniform temperature field throughout the disc. The exponent n is a parameter to control the thickness profile of the disc. A graphical demonstration of the effects of the exponent n, with respect to normalized radius $\rho = r/b_0$, is shown in Fig. 2, with the assumption of $a = a_0/b_0 = 0.3$. We remark that when $r = a_0$, $h/h_0 = 1$, regardless of n. It can be seen that for $n = 0$ the disc has a uniform thickness everywhere. For $n > 0$, the thickness close to the disc center is smaller, and vice versa.

The disc has no stress at the initial instant. The increase in temperature from its initial value, T, and the constraints imposed on the disc affects the zero stress state. It is natural to introduce a cylindrical coordinate system (r, θ, z) with its z- axis coinciding with the axis of symmetry of the disc. Symmetry dictates that the normal stresses in this coordinate system, σ_r, σ_θ and σ_z, are the principal stresses and the circumferential displacement vanishes everywhere. The radial displacement is denoted by u. It is supposed that the state of stress is plane ($\sigma_z = 0$) and the strains are infinitesimal. Plastic yielding is controlled by the von Mises yield criterion. In the case under consideration this criterion can be written as

$$\sigma_r^2 + \sigma_\theta^2 - \sigma_\theta \sigma_r = \sigma_Y^2, \tag{2}$$

where σ_Y is the yield stress in uniaxial tension. The classical Duhamel-Neumann law is adopted. In particular, the elastic portions of the total strains are related to the stresses as

$$\varepsilon_r^e = \frac{\sigma_r - \nu\sigma_\theta}{E}, \quad \varepsilon_\theta^e = \frac{\sigma_\theta - \nu\sigma_r}{E}, \quad \varepsilon_z^e = -\frac{\nu\left(\sigma_r + \sigma_\theta\right)}{E}, \tag{3}$$

where E is Young's modulus and ν is Poisson's ratio. The thermal portions of the total strains are given by

$$\varepsilon_r^T = \varepsilon_\theta^T = \varepsilon_z^T = \alpha T \ , \tag{4}$$

where α is the coefficient of linear thermal expansion in units of meter per meter and per ˚C, or 1/˚C. The total strains in plastic regions are

$$\varepsilon_r = \varepsilon_r^T + \varepsilon_r^e + \varepsilon_r^p, \quad \varepsilon_\theta = \varepsilon_\theta^T + \varepsilon_\theta^e + \varepsilon_\theta^p, \quad \varepsilon_z = \varepsilon_z^T + \varepsilon_z^e + \varepsilon_z^p \quad , \tag{5}$$

where ε_r^p, ε_θ^p and ε_z^p are the plastic portions of the total strains. In the case under consideration, the total radial and circumferential strains are

$$\varepsilon_r = \frac{\partial u}{\partial r}, \quad \varepsilon_\theta = \frac{u}{r} \ , \tag{6}$$

The flow theory of plasticity is adopted. Therefore, the associated flow rule connects stresses and strain rates rather than strains. Since the strains are infinitesimal, the components of the strain rate tensor are obtained as the local time derivatives of the corresponding components of the strain tensor. However, since the material model is rate-independent, these time derivatives can be replaced with the corresponding derivatives with respect to any other monotonically increasing parameter. Denote this parameter by p. Then,

$$\begin{aligned}
&\zeta_r = \frac{\partial \varepsilon_r}{\partial p}, \quad \zeta_\theta = \frac{\partial \varepsilon_\theta}{\partial p}, \quad \zeta_z = \frac{\partial \varepsilon_z}{\partial p}, \\
&\zeta_r^e = \frac{\partial \varepsilon_r^e}{\partial p}, \quad \zeta_\theta^e = \frac{\partial \varepsilon_\theta^e}{\partial p}, \quad \zeta_z^e = \frac{\partial \varepsilon_z^e}{\partial p}, \\
&\zeta_r^p = \frac{\partial \varepsilon_r^p}{\partial p}, \quad \zeta_\theta^p = \frac{\partial \varepsilon_\theta^p}{\partial p}, \quad \zeta_z^p = \frac{\partial \varepsilon_z^p}{\partial p}.
\end{aligned} \tag{7}$$

The associated flow rule gives

$$\zeta_r^p = \lambda\left(2\sigma_r - \sigma_\theta\right), \quad \zeta_\theta^p = \lambda\left(2\sigma_\theta - \sigma_r\right), \quad \zeta_z^p = -\lambda\left(\sigma_r + \sigma_\theta\right), \tag{8}$$

where $\lambda \geq 0$. It is supposed that σ_Y, E and γ are dependent of temperature whereas ν is not. Temperature-independent (TI) Poisson's ratio is a reasonable assumption for many materials (Noda 1991). The temperature-dependent properties are represented as

$$E = E_0 f_E\left(T\right), \quad \alpha = \alpha_0 f_\alpha\left(T\right), \quad \sigma_Y = \sigma_0 f_\sigma\left(T\right), \tag{9}$$

where E_0, α_0, and σ_0 are constants whereas $f_E(T)$, $f_\alpha(T)$, and $f_\sigma(T)$ are prescribed functions of T. With no loss of generality, it is possible to put $f_E(0) = f_\alpha(0) = f_\sigma(0) = 1$.

It is convenient to introduce the following dimensionless quantities

$$\rho = \frac{r}{b_0} \quad \text{and} \quad a = \frac{a_0}{b_0}. \tag{10}$$

Using (1) the only non-trivial equilibrium equation is

$$\rho \frac{\partial \sigma_r}{\partial \rho} + \left(1+n\right)\sigma_r = \sigma_\theta \ . \tag{11}$$

The boundary conditions are

$$\sigma_r = 0, \tag{12}$$

for $\rho = a$ and $u = 0$ for $\rho = 1$. It is evident from (6) that the latter is equivalent to

$$\varepsilon_\theta = 0 \ , \tag{13}$$

for $\rho = 1$.

2.2 Elastic solution

In the following, the elastic solution and the initiation of plastic yielding are developed. In the case of axisymmetric plane stress problems the general thermo-elastic solution is

$$\frac{\sigma_r}{\sigma_Y} = A\rho^{\gamma_1} + B\rho^{\gamma_2}, \quad \frac{\sigma_\theta}{\sigma_Y} = A\left(1+n+\gamma_1\right)\rho^{\gamma_1} + B\left(1+n+\gamma_2\right)\rho^{\gamma_2} \ . \tag{14}$$

$$\begin{aligned}
\frac{\varepsilon_r}{k} &= A\left[1-\left(1+n+\gamma_1\right)\nu\right]\rho^{\gamma_1}+B\left[1-\left(1+n+\gamma_2\right)\nu\right]\rho^{\gamma_2}+\tau,\\
\frac{\varepsilon_\theta}{k} &= A\left(1+n-\nu+\gamma_1\right)\rho^{\gamma_1}+B\left(1+n-\nu+\gamma_2\right)\rho^{\gamma_2}+\tau,\\
\frac{\varepsilon_z}{k} &= -\nu\left[A\left(2+n+\gamma_1\right)\rho^{\gamma_1}+B\left(2+n+\gamma_2\right)\rho^{\gamma_2}\right]+\tau.
\end{aligned} \tag{15}$$

where A and B are constants of integration and

$$\begin{aligned}
&k=\frac{\sigma_Y}{E},\quad \tau=\frac{\alpha T}{k},\\
&\gamma_1=-\left(1+\frac{n}{2}\right)-\frac{1}{2}\sqrt{\left(2-n\right)^2+4n\left(1-\nu\right)},\\
&\gamma_2=-\left(1+\frac{n}{2}\right)+\frac{1}{2}\sqrt{\left(2-n\right)^2+4n\left(1-\nu\right)}
\end{aligned} \tag{16}$$

When the entire disc is elastic, A and B are determined from (12) and (13) as

$$\begin{aligned}
A=A_e&=-\frac{\tau a^{\gamma_2}}{\left(1+n-\nu+\gamma_1\right)a^{\gamma_2}-\left(1+n-\nu+\gamma_2\right)a^{\gamma_1}},\\
B=B_e&=\frac{\tau a^{\gamma_1}}{\left(1+n-\nu+\gamma_1\right)a^{\gamma_2}-\left(1+n-\nu+\gamma_2\right)a^{\gamma_1}}.
\end{aligned} \tag{17}$$

Substituting (14) at $\rho = a$ into (2) and using (17) it is possible to find the value of τ corresponding to the initiation of the plastic zone as

$$\tau_e=\frac{a^{\gamma_2}\left(1+\gamma_1+n-\nu\right)-a^{\gamma_1}\left(1+\gamma_2+n-\nu\right)}{a^{\gamma_1}a^{\gamma_2}\left(\gamma_1-\gamma_2\right)}. \tag{18}$$

Then, substituting (17) and (18) into (14) yields the following value of the stress σ_θ at $\rho = a$ and $\tau = \tau_e$

$$\sigma_\theta=-\sigma_Y. \tag{19}$$

2.3 Elastic/plastic stress solution

As for the elastic/plastic stress solution, the yield criterion (2) is satisfied by the following substitution

$$\frac{\sigma_r}{\sigma_Y}=-\frac{2\sin\psi}{\sqrt{3}},\quad \frac{\sigma_\theta}{\sigma_Y}=-\frac{\sin\psi}{\sqrt{3}}-\cos\psi\ , \tag{20}$$

where ψ is a new unknown function of p and ρ. The plastic zone propagates from the hole toward

to outer rim. Therefore, the stresses given in (20) must satisfy the boundary condition (12), and substituting (20) into (11) gives

$$2\rho\cos\psi\frac{\partial\psi}{\partial\rho}-\sqrt{3}\cos\psi+\left(1+2n\right)\sin\psi=0\,. \tag{21}$$

Using (12) and (19) it is possible to find from (20) that $\psi = 0$ at $\rho = a$. Solving (21) with the use of this boundary condition results in

$$\begin{aligned}&\frac{\rho}{a}=\exp\left[\frac{\sqrt{3}\psi}{2\left(1+n+n^2\right)}\right]\left[\cos\psi-\frac{\left(1+2n\right)}{\sqrt{3}}\sin\psi\right]^{\beta},\\&\beta=-\frac{1+2n}{2\left(1+n+n^2\right)}\end{aligned} \tag{22}$$

Let ψ_c be the value of ψ at the elastic/plastic boundary, $\rho = \rho_c$. Then, it follows from (22) that

$$\frac{\rho_c}{a}=\exp\left[\frac{\sqrt{3}\psi_c}{2\left(1+n+n^2\right)}\right]\left[\cos\psi_c-\frac{\left(1+2n\right)}{\sqrt{3}}\sin\psi_c\right]^{\beta}. \tag{23}$$

Both σ_r and σ_θ are continuous across the elastic/plastic boundary. The distribution of the stresses in the elastic zone is given by (14). Then, combining (14) and (20) results in

$$\begin{aligned}&A\rho_c^{\gamma_1}+B\rho_c^{\gamma_2}=-\frac{2\sin\psi_c}{\sqrt{3}},\\&A\left(1+n+\gamma_1\right)\rho_c^{\gamma_1}+B\left(1+n+\gamma_2\right)\rho_c^{\gamma_2}=-\frac{\sin\psi_c}{\sqrt{3}}-\cos\psi_c.\end{aligned} \tag{24}$$

These equations along with (23) are used to express A and B in terms of ψ_c as

$$\begin{aligned}&A=\frac{1}{\sqrt{3}}\left[\frac{\sqrt{3}\cos\psi_c-\left(1+2n+2\gamma_2\right)\sin\psi_c}{\gamma_2-\gamma_1}\right]\rho_c^{-\gamma_1},\\&B=-\frac{1}{\sqrt{3}}\left[\frac{\sqrt{3}\cos\psi_c-\left(1+2n+2\gamma_1\right)\sin\psi_c}{\gamma_2-\gamma_1}\right]\rho_c^{-\gamma_2}\end{aligned} \tag{25}$$

Here ρ_c should be eliminated by means of (23). Combining the boundary condition (13) and the solution (15) for ε_θ gives

$$\tau=-\left(1+n-\nu+\gamma_1\right)A-\left(1+n-\nu+\gamma_2\right)B\,. \tag{26}$$

Eliminating A and B in (26) by means of (25) leads to

$$\tau = -\frac{\left(1+n-\nu+\gamma_1\right)}{\sqrt{3}}\left[\frac{\sqrt{3}\cos\psi_c-\left(1+2n+2\gamma_2\right)\sin\psi_c}{\gamma_2-\gamma_1}\right]\rho_c^{-\gamma_1}+ \\ +\frac{\left(1+n-\nu+\gamma_2\right)}{\sqrt{3}}\left[\frac{\sqrt{3}\cos\psi_c-\left(1+2n+2\gamma_1\right)\sin\psi_c}{\gamma_2-\gamma_1}\right]\rho_c^{-\gamma_2} \tag{27}$$

The entire disc becomes plastic when $\rho_c = 1$. The corresponding values of ψ_c and τ are denoted by ψ_p and τ_p, respectively. The equation for ψ_p follows from (23) as

$$1 = a\exp\left[\frac{\sqrt{3}\psi_p}{2\left(1+n+n^2\right)}\right]\left[\cos\psi_p-\frac{\left(1+2n\right)}{\sqrt{3}}\sin\psi_p\right]^{\beta}. \tag{28}$$

The value of τ_p is determined from (27) at $\psi_c = \psi_p$ as

$$\tau_p = -\frac{\left(1+n-\nu+\gamma_1\right)}{\sqrt{3}}\left[\frac{\sqrt{3}\cos\psi_p-\left(1+2n+2\gamma_2\right)\sin\psi_p}{\gamma_2-\gamma_1}\right]+ \\ +\frac{\left(1+n-\nu+\gamma_2\right)}{\sqrt{3}}\left[\frac{\sqrt{3}\cos\psi_p-\left(1+2n+2\gamma_1\right)\sin\psi_p}{\gamma_2-\gamma_1}\right] \tag{29}$$

The normalized temperature is defined as follows to measure the difference between elastic-reversible and plastic-collapse temperatures.

$$\delta\tau = \frac{T_p - T_e}{T_e}. \tag{30}$$

When $T < T_e$, purely elastic responses can be obtained when the thermal loading is removed. When $T = T_p$ or $T > T_p$, the whole disc is plastically deformed. The normalized temperature indicates the range of temperature for the disc to go from purely elastic deformation ($T = T_e$) up to plastic collapse ($T = T_p$).

2.4 Elastic/plastic strain solution at $\tau_e \le \tau \le \tau_p$ (or $0 \ge \psi_c \ge \psi_p$)

Consider the plastic zone. Eliminating λ in Eq. (8) and using Eq. (20) yield

$$2\cos\psi\zeta_r^p = \left(\sqrt{3}\sin\psi-\cos\psi\right)\zeta_\theta^p, \quad 2\cos\psi\zeta_z^p = -\left(\cos\psi+\sqrt{3}\sin\psi\right)\zeta_\theta^p \tag{31}$$

or

$$2\cos\psi\frac{\partial\varepsilon_r^p}{\partial p} = \left(\sqrt{3}\sin\psi-\cos\psi\right)\frac{\partial\varepsilon_\theta^p}{\partial p}, \quad 2\cos\psi\frac{\partial\varepsilon_z^p}{\partial p} = -\left(\cos\psi+\sqrt{3}\sin\psi\right)\frac{\partial\varepsilon_\theta^p}{\partial p}. \tag{32}$$

It is evident from Eq. (22) that ψ is independent of p. Therefore, the above equations can be readily re-written as

$$2\cos\psi\varepsilon_r^p=\left(\sqrt{3}\sin\psi-\cos\psi\right)\varepsilon_\theta^p,\quad 2\cos\psi\varepsilon_z^p=-\left(\cos\psi+\sqrt{3}\sin\psi\right)\varepsilon_\theta^p. \tag{33}$$

This solution satisfies the condition that all the plastic strains vanish simultaneously. In particular, it is evident that the condition that all the plastic strains vanish at the elastic-plastic boundary is equivalent to the condition that one of these strains vanishes. It is seen from Eq. (31) and Eq. (33) that there is no difference between the deformation and flow theories of plasticity in the case under consideration. It follows from Eq. (6) that the equation of strain compatibility is $\rho\partial\varepsilon_\theta/\partial\rho=\varepsilon_r-\varepsilon_\theta$. Using Eq. (4) and Eq. (5) this equation transforms to

$$\rho\frac{\partial\varepsilon_\theta^e}{\partial\rho}+\rho\frac{\partial\varepsilon_\theta^p}{\partial\rho}=\varepsilon_r^e+\varepsilon_r^p-\varepsilon_\theta^e-\varepsilon_\theta^p. \tag{34}$$

Substituting Eq. (20) into Eq. (3) gives the elastic portion of the strain tensor in the form

$$\begin{aligned}&\varepsilon_r^e=k\left[\nu\cos\psi-\frac{(2-\nu)}{\sqrt{3}}\sin\psi\right],\quad \varepsilon_\theta^e=-k\left[\cos\psi+\frac{(1-2\nu)}{\sqrt{3}}\sin\psi\right],\\&\varepsilon_z^e=k\nu\left(\cos\psi+\sqrt{3}\sin\psi\right).\end{aligned} \tag{35}$$

Substituting Eq. (33) and Eq. (35) into Eq. (34) and replacing differentiation with respect to ρ with differentiation with respect to ψ by means of Eq. (21) yield

$$\begin{aligned}&\frac{\partial\varepsilon_\theta^p}{\partial\psi}-\frac{\sqrt{3}\left(\sin\psi-\sqrt{3}\cos\psi\right)}{\sqrt{3}\cos\psi-(1+2n)\sin\psi}\varepsilon_\theta^p=k\Lambda(\psi),\\&\Lambda(\psi)=\frac{2(1+\nu)\cos\psi\left(\sqrt{3}\cos\psi-\sin\psi\right)}{\sqrt{3}\left[\sqrt{3}\cos\psi-(1+2n)\sin\psi\right]}+\frac{(1-2\nu)}{\sqrt{3}}\cos\psi-\sin\psi\end{aligned}. \tag{36}$$

This is a linear differential equation for ε_θ^p. Therefore, its general solution can be found by well known methods, as follows. The general solution of the first-order ordinary differential equation with the form of

$$\frac{\partial\varepsilon_\theta^e}{\partial\psi}+f(\psi)\frac{\partial\varepsilon_\theta^p}{\partial\psi}=g(\psi), \tag{37}$$

where $f(\psi)$ and $g(\psi)$ are arbitrary functions, can be written as

$$\varepsilon_\theta^e(\psi)=e^{-\int f(x)dx}\left(\int_{\psi_c}^{\psi}g(x)e^{\int f(x)dx}dx+c\right). \tag{38}$$

Here c is a to-be-determined constant with boundary condition, x is a dummy variable of integration, and $\psi=\psi_c$ is the lower bound of the integration domain. Further manipulations yield that the solution of Eq. (36), in which the c coefficient is determined from the boundary condition

$\varepsilon_\theta^p = 0$ for $\psi = \psi_c$, is

$$\varepsilon_\theta^p = kV\left(\psi,\psi_c\right)U\left(\psi,\psi_c\right),$$
$$V\left(\psi,\psi_c\right) = \exp\left[-\frac{\sqrt{3}}{2}\frac{\left(2+n\right)}{\left(1+n+n^2\right)}\left(\psi-\psi_c\right)\right]\left[\frac{\sqrt{3}\cos\psi-\left(1+2n\right)\sin\psi}{\sqrt{3}\cos\psi_c-\left(1+2n\right)\sin\psi_c}\right]^\mu,$$
$$U\left(\psi,\psi_c\right) = \int_{\psi_c}^{\psi}\Lambda\left(x\right)\exp\left[\frac{\sqrt{3}}{2}\frac{\left(2+n\right)}{\left(1+n+n^2\right)}\left(x-\psi_c\right)\right]\left[\frac{\sqrt{3}\cos\psi_c-\left(1+2n\right)\sin\psi_c}{\sqrt{3}\cos x-\left(1+2n\right)\sin x}\right]^\mu dx, \quad (39)$$
$$\mu = \frac{3n}{2\left(1+n+n^2\right)}$$

Here x is a dummy variable of integration. The other plastic strain components may be determined from Eqs. (33) and (39). Using Eqs. (16) and (27), Eq. (4) can be rewritten in the form

$$\varepsilon_r^T = \varepsilon_\theta^T = \varepsilon_z^T = -k\left(1+n-\nu+\gamma_1\right)\rho_c^{-\gamma_1}\left[\cos\psi_c-\frac{\sin\psi_c}{\sqrt{3}}\left(2\gamma_2+1+2n\right)\right]\left(\gamma_2-\gamma_1\right)^{-1}-$$
$$-k\left(1+n-\nu+\gamma_2\right)\rho_c^{-\gamma_2}\left[-\cos\psi_c+\frac{\sin\psi_c}{\sqrt{3}}\left(2\gamma_1+1+2n\right)\right]\left(\gamma_2-\gamma_1\right)^{-1}. \quad (40)$$

It is seen from Eqs. (5), (35), (39) and (40) that all the strain components are proportional to k. Thus, simple scaling of a single solution for a disc of given a – value and Poisson's ratio supplies the solutions for similar discs of material with the same Poisson's ratio but any temperature-dependent yield stress and Young's modulus. Also, the value of α is not involved in the solution in terms of τ. However, both k and α are necessary to find the physical temperature according to Eqs. (9) and (16). The solution found provides the radial distribution of strains in the plastic zone in parametric form with ψ being the parameter varying in the range $0 \le \psi \le \psi_c$. In particular, the total strains are found from Eqs. (5), (33), (35), (39), and (40). In the elastic zone, the total strains are given by Eq. (15) where A and B should be eliminated by means of Eq. (25).

2.5 Elastic/plastic strain solution at $\tau_p \le \tau$.

Eqs. (22), (33), (35) and (36) are valid in the range $a \le \rho \le 1$. Using Eq. (16), Eq. (4) can be rewritten in the form

$$\varepsilon_r^T = \varepsilon_\theta^T = \varepsilon_z^T = k\tau. \quad (41)$$

Let ψ_b be the value of ψ at $\rho = 1$. Then, substituting Eqs. (35) and (41) into Eq. (5) and the resulting expression for ε_θ into the boundary condition Eq. (13) give the following algebraic equation.

$$0 = \varepsilon_\theta\left(\rho=1\right) = \kappa\tau - k\left(\cos\psi_b + \frac{1-2\nu}{\sqrt{3}}\sin\psi_b\right) + \varepsilon_\theta^p\left(\psi_b\right). \quad (42)$$

Re-ordering the above equation yields the plastic hoop strain at the outer rim.

$$\varepsilon_\theta^p = k\left[\cos\psi_b + \frac{(1-2\nu)}{\sqrt{3}}\sin\psi_b\right] - k\tau\,, \tag{43}$$

at $\rho = 1$ (or $\psi = \psi_b$). Moreover, it follows from Eq. (22) that

$$\frac{1}{a} = \exp\left[\frac{\sqrt{3}\psi_b}{2\left(1+n+n^2\right)}\right]\left[\frac{\sqrt{3}\cos\psi_b - (1+2n)\sin\psi_b}{\sqrt{3}}\right]^\beta. \tag{44}$$

Thus the value of ψ_b does not change with temperature at $\tau_p \le \tau$. Since $\psi_b = \psi_p$ is the initial condition at $\tau_p = \tau$, it is evident that $\psi_b = \psi_p$ in the range $\tau_p \le \tau$. The solution of Eq. (36) satisfying the boundary condition Eq. (43), with the help of general solution Eq. (38) to determine the c coefficient, is

$$\frac{\varepsilon_\theta^p}{k} = V\left(\psi,\psi_p\right)\left[U\left(\psi,\psi_p\right) + \cos\psi_p + \frac{(1-2\nu)}{\sqrt{3}}\sin\psi_p - \tau\right]. \tag{45}$$

This solution replaces the solution Eq. (39). The other plastic strain components are determined from Eqs. (33) and (45). Thus the radial distribution of the plastic strains has been determined in parametric form with ψ being the parameter varying in the range $0 \le \psi \le \psi_p$. Having the solution for the plastic strains the total strains are immediately found from Eqs. (5), (33), (35), (41), and (45).

3. Examples and discussion

In our numerical examples of the above derived analytical results, the high-strength low-alloy steel is chosen, and its time-dependent material functions $f_E(T)$, $f_\alpha(T)$, and $f_\sigma(T)$ in the range $0 \le T \le 400$ ˚C are as follows.

$$\begin{aligned} f_E\left(T\right) &= 1 + \frac{T}{2000\ln\left(T/1100\right)}, \\ f_\sigma\left(T\right) &= 1 + \frac{T}{600\ln\left(T/1630\right)}, \\ f_\alpha\left(T\right) &= 1 + 2.56\times10^{-4}T + 2.14\times10^{-7}T^2, \end{aligned} \tag{46}$$

where the temperature difference T is in ˚C and the initial temperature is 20˚C (Argeso and Eraslan 2008). In other words, when $T = 0$, the temperature is the initial temperature. In addition, $E_0 = 200$GPa, $\sigma_0 = 410$MPa, $\nu = 0.3$, and $\alpha_0 = 11.7 \times 10^{-6}$ meters per meter and per ˚C (i.e., 1/˚C). We remark that temperature-dependent material properties are assumed throughout the calculated examples, except stated otherwise.

Using these functions the temperature variation, Fig. 3 shows the normalized temperature $\delta\tau$ versus normalized radius a, as calculated from Eq. (30), for various hyperbolic profile n. The

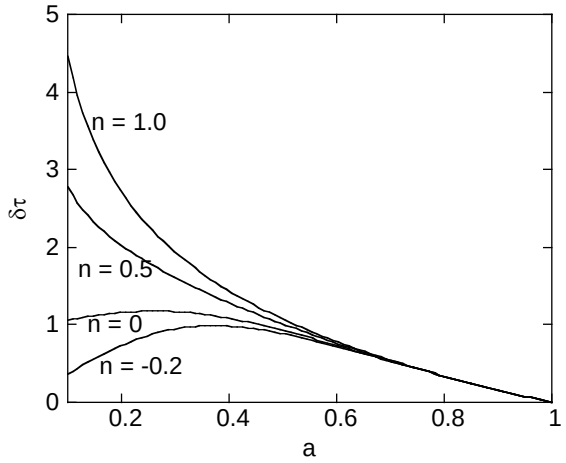

Fig. 3 Normalized temperature, $\delta\tau$ versus normalized radius, a, for various hyperbolic profile n, calculated from Eq. (30)

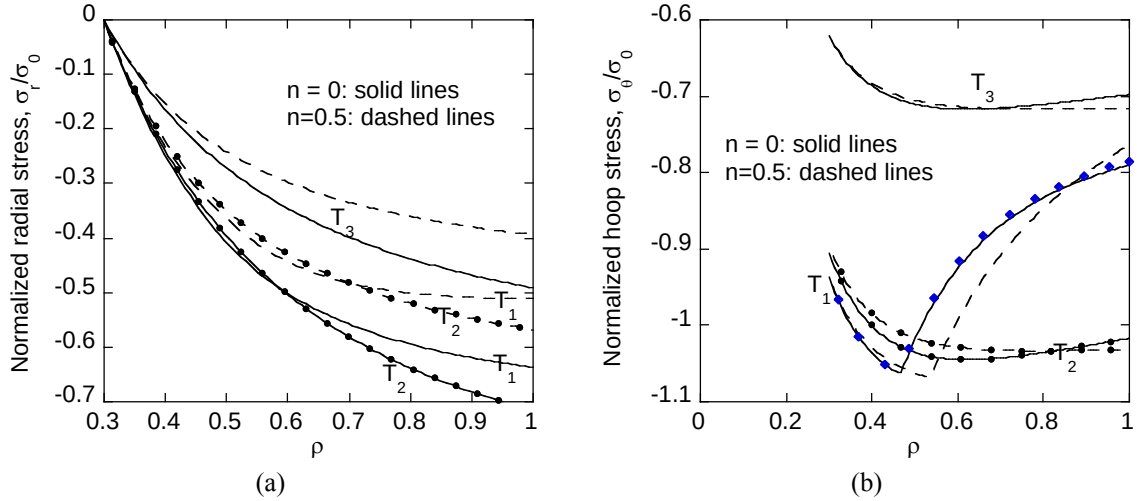

Fig. 4 Stress distribution along the radius for the n = 0 and n = 0.5 case. (a) Radial stress, and (b) circumferential stress. The normalization was with respect to σ_0. Solid circular dots indicate the plastic-collapse case (i.e., $T = T_2$). Blue diamonds are finite element solutions for comparison

physical meaning of the normalized temperature is the temperature range of the disc will experience above T_e (upper temperature limit for purely elastic deformation) but smaller than T_p (plastic collapse, i.e., plastic deformation everywhere in the disc). It can be seen that for large hole size (a greater than about 0.6), $\delta\tau$ linearly decreases as a increases, regardless of the n value. In other words, thickness variations do not play a role for discs with a large hole in the middle. For small holes, a less than about 0.4, positive n values will lead to large $\delta\tau$, while negative n values reduce the temperature range. Physically, negative n values result in larger thickness around the hole, and once it is in plastic zone due to temperature increase, the whole disc will go into plastic deformation with a slightly additional temperature increase.

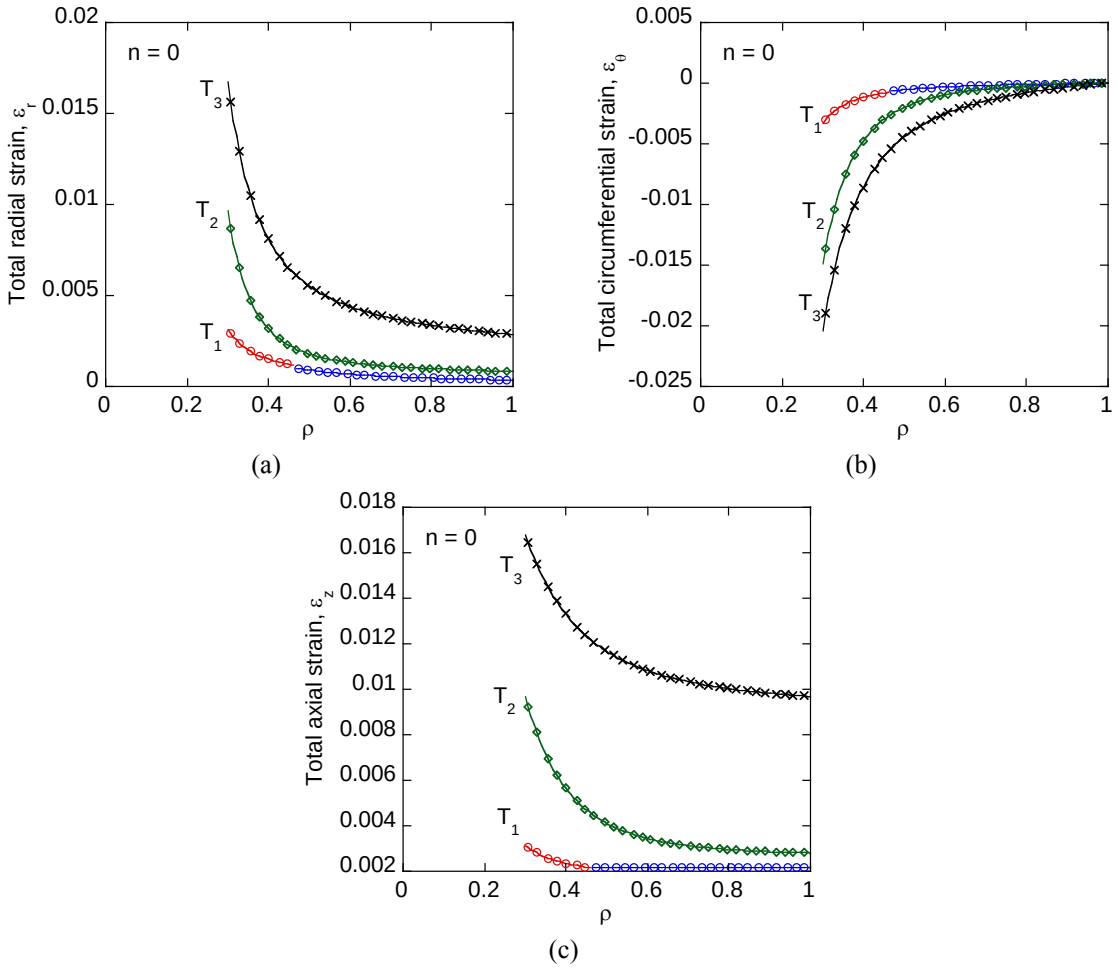

Fig. 5 Demonstration of strain distributions along the radius for the $n = 0$ case. (a) Radial strain, (b) circumferential strain and (c) axial strain, i.e., the strain along the thickness direction

Figs. 4 and 5, respectively, show the stress and strain distribution to delineate how the stress and strain vary along the radial direction. In Fig. 4, both $n = 0$ and $n = 0.5$ case are shown for demonstrating profile effects. Three temperature differences are adopted, $T_1 = 104.26^\circ$C, $T_2 = 139.95^\circ$C and $T_3 = 350^\circ$C. For $n = 0$, the T_e and T_p are 68.57 $^\circ$C and 139.95°C, respectively. Hence, when $T_e < T_1 < T_p$, an elastic-plastic boundary may exist in the disc. When $T = T_2$, plastic collapse of the whole disc occurs, and filled circular dots are placed on the curves. The radial and circumferential stress, normalized with respect to σ_0, are plotted in Figs. 4(a) and (b), respective. It can be seen that both stresses are compressive. For radial stress, as ρ increases, the stress magnitude increases, i.e., the radial stress becomes more negative. However, this monotonicity does not occur for the circumferential stress. To somewhat justify our analytical solutions, finite element results (blue diamond markers) for the hoop stress are shown for the $T = T_1$ case. In the finite element analysis, the yield stress is modified in accordance with Eq. (42); all other material properties were assumed to be temperature independent. The progression of the hoop stress is

consistent between our analytical solution and finite element results. Finite element data for the trend of the radial stress versus radius is identical to that obtained by our analytical solutions, and they are not shown here for clear presentation of Fig. 4(a). Detailed of our finite element analysis can be found later in the text before the Conclusion section. We emphasize that finite element solutions contain numerical and discretization errors.

When $T = T_1$, part of the disc is still in the purely elastic state, and the elastic-plastic boundary is at about $\rho = 0.45$, where the radial stress is continuous through the elastic-plastic boundary, but the circumferential stress around the elastic-plastic boundary becomes non-differentiable. In addition, if the material's yield stress is temperature independent, the normalized hoop stress at the inner rim of the disc is equal to -1. As for the thickness profile effects, it can be seen in Figs. 4(a) and (b), the radial stress is reduced in this particular choice of the $n = 0.5$ profile due to additional material around the outer rim to lower stresses. Furthermore, the elastic-plastic boundary moves toward outer rim as n increases from 0 to 0.5, as shown by the turning point in the hoop stress for the $T = T_1$ case. Hence, larger plastic zone in the $n = 0.5$ case.

The total radial strain, circumferential strain and axial strain (i.e., along the Z axis) are shown in Figs. 5(a), (b) and (c), respectively, for the $n = 0$ case. It can be seen that the total circumferential strain reaches zero at $\rho = 1$, as expected. Larger temperatures result in larger magnitudes in all strain components.

In order to examine the effects of the thickness variations with the derived analytical solutions here, Fig. 6 shows the comparisons on circumferential strain for two different temperatures, namely $T = 106.3^{\circ}$C and $T = 350^{\circ}$C. Three n values are calculated, $n_1 = -0.2$, $n_2 = 0$ and $n_3 = 0.5$. It is noted that the plastic collapse temperature T_p depends on the n values. Hence, the three n's lead to the following three plastic collapse temperatures 132.49˚C, 139.95˚C and 150.31˚C for $n = -0.2$, 0 and 0.5, respectively. The corresponding T_e's are 71.69˚C, 68.57˚C, 62.28˚C also for $n = -0.2$, 0 and 0.5, respectively. In Fig. 6(a), $T > T_e$, but less than T_p for all n's. It can be seen that as n increases from negative values to positive values, the circumferential strain becomes more negative. In other words, the strain for $n > 0$ is more negative, i.e., larger, than the strain for $n = 0$. However, the strain for $n < 0$ is less negative, i.e., smaller than the strain for $n = 0$. When comparing Fig. 6(a) and (b), this relationship is reversed. In other words, when $T = 350^{\circ}$C, which makes the disc plastically deformed everywhere, $n < 0$ results in an increase in strain.

As for the effects of the temperature-dependent (TD) material properties, Figs. 7(a) and (b) show comparisons on the circumferential strain for $n = 0$ and $n = 0.5$, respectively, at the three temperatures. It can be seen that when $n = 0$, the disc has uniform thickness, the effects of the temperature dependent material properties are minor. However, the combined effects of the thickness variations and temperature-dependent (TD) material properties show stronger effects, particularly at high temperatures, i.e., $T = T_3$. Therefore, in real-world applications, the considerations of temperature-dependent (TD) material properties are crucial when thickness variations are present.

In both of Figs. 6 and 7, as well as Fig. 4(b), numerical data, shown as blue diamonds, were obtained by the finite element analysis with the commercial software COMSOL (2013) for the $T = T_1$ case with $n = 0$ and 0.5. The assumption of temperature-independent (TI) material properties was adopted in the numerical analysis, along with the von Mises yield criterion in the elastic-perfectly plastic material model. Reasonable agreements are obtained between our analytical solution and the finite element results. We remark that the finite element model was three-dimensional with axisymmetric assumptions for the annular plate under a uniform temperature increase. Its inner and outer radius are 0.3 m and 1 m, respectively. The plate thickness at the inner

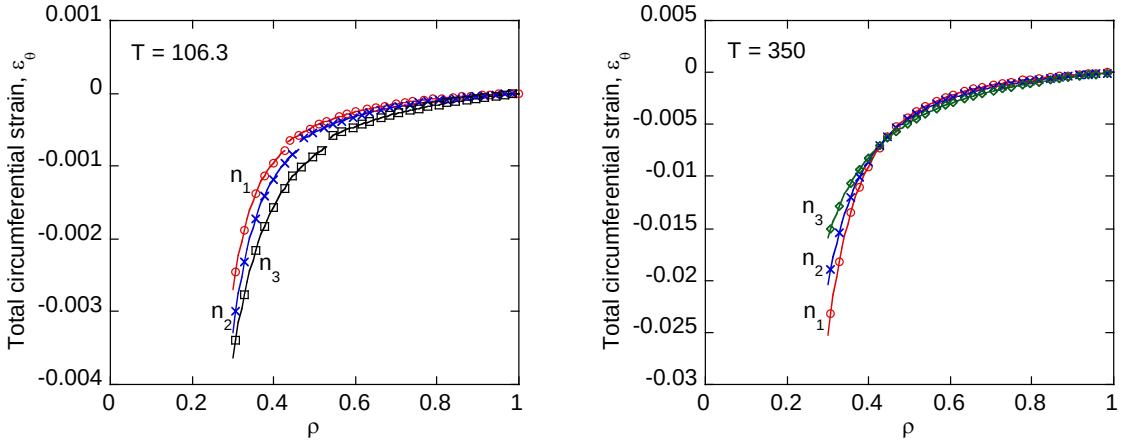

(a) (b)

Fig. 6 Effects of the thickness variations for (a) $T = 106.3^{\circ}\mathrm{C} < T_p$, and (b) $T = 350^{\circ}\mathrm{C} > T_p$

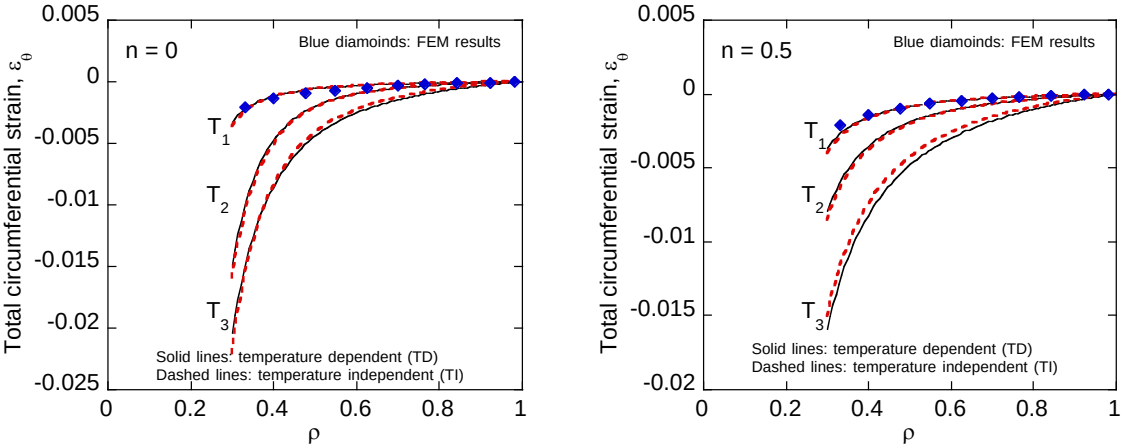

(a) (b)

Fig. 7 Effects of the temperature-dependent material properties for (a) $n = 0$ and (b) $n = 0.5$

rim is 0.05 m. The chosen geometry is to mimic the two-dimensional plane stress theoretical solutions developed here. A quadratic triangular element was adopted, and the total number of elements was 1559 with the average quality of 0.9852. The difference between the finite element model and our theoretical model is acknowledged, and comparisons between them should only be made qualitatively, due to model differences, as well as numerical and discretization error inherently in the finite element method.

As pointed out by many authors (Lippmann 1992, Kovacs 1994, Bengeri and Mack 1994) that temperature-dependent yield stress is the most sensitive material property, and hence many reported works in the literature consider only yield strength to be temperature dependent, and set all other material properties to be temperature independent. Metallurgically speaking, all mechanical properties of metallic materials are temperature dependent, but the strengths of their dependences are not on the same magnitude. As temperature increases, changes in the mechanical

properties increase due to heavily altering the microstructures of metallic materials, such as dislocation density, grain boundaries, and possible formation of new phases. In this work, we put forward theoretical developments to obtain analytical solutions that include temperature-dependent Young's modulus, yield strength and thermal expansion coefficient, as well as thickness variations. The functional forms used in this work have the largest temperature sensitivity for yield stress, as illustrated by Argeso and Eraslan (2008). In Fig. 4(b), the finite element solutions (blue diamonds) only consider the temperature-corrected yield stress for $T = T_1$. It can be seen that the finite element results are very close to our analytical solutions, which includes three TD material properties, indicating that considering only temperature-dependent yield strength can capture most of the behavior of the hoop stress. However, from Fig. 7(b), we can see the largest deviation between TD and TI results occur at highest temperature and $n = 0.5$. Therefore, it is conjectured that for moderate or less temperature elevation, considering only TD yield stress may be sufficient. But, for higher temperatures, reductions of elastic constants and changes in thermal expansion coefficient may have significant influences on the stress and strain distributions. Hence, considerations of all material properties to be temperature dependent may be necessary for high-temperature applications. In addition, different materials may have different temperature-dependent material functions, which may have different weights on the strength of the temperature dependence. Therefore, with the theoretical solutions developed here, one can explore a material search to see which materials are better modeled with more material properties being assumed to be temperature dependent.

4. Conclusions

Analytical solutions, in the purely elastic, elastic-plastic and fully plastic situation, of the hollow disk with hyperbolic thickness profile under uniform temperature field have been obtained, including temperature-dependent material properties. The Poisson's ratio of the material is assumed to be temperature independent.

This assumption follows from direct experiment (Noda 1991). On the other hand, it has been hypothesized in (Lippmann 1992, Kovacs 1994, Bengeri and Mack 1994) that it is most important to take into account the effect of temperature on the yield stress whereas other mechanical properties may be assumed temperature-independent. Even though this may be a reasonable assumption for many materials, it is desirable to have a simple method to quantitatively evaluate an additional effect due to the temperature dependence of other thermo-mechanical properties on elastic/plastic solutions. The present solution provides such a benchmark problem. A distinguished feature of this solution is that the dimensionless quantities have been chosen such that the general solution is independent of temperature dependence of thermo-mechanical properties. Indeed, even the solution to Eq. (36), which is the most difficult one among all equations to be solved, is only affected by these properties because of k which is just a multiplier. Therefore, for any given thickness profile of the disc numerical integration can be carried out just one time for all possible variations of thermo-mechanical properties with temperature. The effect of temperature-dependent thermo-mechanical properties is then revealed when the dimensionless quantities are transformed into physical quantities.

In summary, in this work, it is found that the thickness variations, controlled by the n value, have strong effects on the stress and strain distribution, as well as the normalized temperature difference $\delta\tau$. A critical change of $\delta\tau$ behavior is when the normalized hole size a is about 0.6.

When a > 0.6, the curves of $\delta\tau$ versus a are identical regardless of thickness profile. Furthermore, it is shown that the combined effects of thickness variations and the temperature-dependent material properties may cause notable deviations from simple analysis that does not include the two effects, in particular, at higher temperatures.

Acknowledgements

One of the authors, YCW, is grateful for research grants from Taiwan NSC 101-2221-E-006-206 and NSC 102-2221-E-006-172. The research described in this paper has also been partly supported by the grants NSC-99-2218-E-194-003-MY3 and NSH-3842.2012.1. A part of this work was done while Sergei Alexandrov was with National Chung Cheng University (Taiwan) as a research scholar under the recruitment program supported by the National Science Council of Taiwan (contract 99-2811-E-194-009).

References

Alujevic, A., Les, P. and Zupec, J. (1993), "Thermal yield of a rotating hyperbolic disk," *Zeitschrift fur Angewandte Mathematik und Mechanik (ZAMM)*, **73**, T283-T287.

Alexandrov, S., Jeng, Y.R. and Lyamina, E. (2012), "Influence of pressure-dependency of the yield criterion and temperature on residual stresses and strains in a thin disk", *Struct. Eng. Mech.*, **44**, 289-303.

Alexandrova, N. and Alexandrov, S. (2004), "Elastic-plastic stress distribution in a plastically anisotropic rotating disk", *Trans. ASME J. Appl. Mech.*, **71**, 427–429.

Argeso, H. and Eraslan, A.N. (2008), "On the use of temperature-dependent physical properties in thermomechanical calculations for solid and hollow cylinders", *Int. J. Therm. Sci.*, **47**, 136-146.

Bengeri, M. and Mack, W. (1994), "The influence of the temperature dependence of the yield stress on the stress distribution in a thermally assembled elastic-plastic shrink fit", *Acta Mech*., 103, 243-257.

COMSOL website (2013), http://www.comsol.com

Eraslan, A.N. (2002), "Von Mises yield criterion and nonlinearly hardening variable thickness rotating annular disks with rigid inclusion", *Mech. Res. Commun.*, **29**, 339-350.

Eraslan, A.N. (2003), "Elastic-plastic deformations of rotating variable thickness annular disks with free, pressurized and radially constrained boundary conditions", *Int. J. Mech. Sci.*, **45**(4), 643-667.

Eraslan, A.N., Orcan, Y. and Güven, U. (2005), "Elastoplastic analysis of nonlinearly hardening variable thickness annular disks under external pressure", *Mech. Res. Commun.*, **32**(3), 306-315.

Eraslan, A.N. and Orcan, Y. (2002), "On the rotating elastic-plastic solid disks of variable thickness having concave profiles", *Int. J. Mech. Sci.*, **44**(7), 1445-1466.

Gamer, U. (1984), "Elastic-plastic deformation of the rotating solid disk", *Archive Appl. Mech. (Ingenieur Archiv)*, **54**(5), 345-354.

Güven, U. (1998), "Elastic-plastic stress distribution in a rotating hyperbolic disk with rigid inclusion", *Int. J. Mech. Sci.*, **40**(1), 97-109.

Güven, U. and Altay, O. (1998), "Linear hardening solid disk with rigid casing subjected to a uniform heat source", Mech. Res. Comm., 25(6), 679-684.

Horstemeyer, M.F. and Bammann, D.J. (2010), "Historical review of internal state variable theory for inelasticity", *International Journal of Plasticity*, **26**, 1310-1334.

Kovacs, A. (1994), "Thermal stresses in a shrink fit due to an inhomegeneous temperature distribution", Acta Mech., 105, 173-187.

Lenard, J. and Haddow, J.B. (1972), "Plastic collapse speeds for rotating cylinders", *Int J Mech Sci.*, **14**(5), 285-292.

Lippmann, H. (1992), "The effect of temperature cycle on the stress distribution in a shrink fit", *Int. J. Plasticity*, 8, 567-582.

Noda., N. (1991), "Thermal stresses in materials with temperature-dependent properties", *Appl. Mech. Rev.*, **44**, 383-397.

Orcan, Y. and Gamer ,U. (1994), "On the expansion of plastic regions in the annular parts of a shrink fit during assemblage", *Z. Angew. Math. Mech*., **74**, 25-35.

Rees, D.W.A. (1999), "Elastic-plastic stresses in rotating disks by von Mises and Tresca", *Zeitschrift fur Angewandte Mathematik und Mechanik (ZAMM)*, **79**(4), 281-288.

Thompson, A.S. and Lester, P.A. (1946), "Stresses in rotating disks at high temperatures", *J. Appl. Mech.*, **13**, A45-A52.

Vivio, F. and Vullo, L. (2010), "Elastic-plastic analysis of rotating disks having non-linearly variable thickness: residual stresses by overspeeding and service stress state reduction", *Ann. Solid Struct. Mech.*, **1**, 87-102.

Withers., P.J. (2007), "Residual stress and its role in failure", *Rep. Prog. Phys.*, **70**, 2211-2264.

You, L.H. and Zhang, J.J. (1999), "Elastic-plastic stresses in a rotating solid disk", *Int. J. Mech. Sci.*, **41**(3), 269-282.

Zimmerman, R.W. and Lutz, M.P. (1999), "Thermal stresses and thermal expansion in a uniformly heated functionally graded cylinder", *J. Therm. Stresses*, **22**, 177-188.